



Enhanced tunability of sandwich-like structural barium strontium titanate thin films on stainless steel substrates

Hanting Dong¹, Guoping Lu¹, Dengren Jin¹, Jianguo Chen¹, and Jinrong Cheng^{1,*}

¹ School of Materials Science and Engineering, Shanghai University, No. 99 Shangda Road, Shanghai 200444, People's Republic of China

Received: 8 May 2016

Accepted: 21 May 2016

Published online:

3 June 2016

© Springer Science+Business Media New York 2016

ABSTRACT

Barium strontium titanate (BST) thin films deposited on stainless steel (SS) substrates can be expected for their potential applications in MEMS-structure tunable microwave devices. In this paper, two sandwich-like structures with varied average Ba/Sr ratio of BST thin films, $\text{Ba}_{0.6}\text{Sr}_{0.4}\text{TiO}_3$ layer in the middle or at ends, on LaNiO_3 buffered SS substrates were fabricated by sol-gel technique, and meanwhile were theoretically carried out via a modified phenomenological model. Results show that dielectric constant and tunability of such BST films can be tailored by average Ba/Sr ratio and structures. When the average Ba/Sr ratio is unchanged, the structure with smaller lattice parameter of middle layer than that of top/bottom layer can achieve larger tunability resulting from its smaller compressive misfit strain, which has been qualitatively characterized by X-ray diffraction and Raman spectra. Especially, the largest tunability reaches 30 % under the electric field of 300 kV cm^{-1} by locating $\text{Ba}_{0.4}\text{Sr}_{0.6}\text{TiO}_3$ layer in the middle and $\text{Ba}_{0.6}\text{Sr}_{0.4}\text{TiO}_3$ layers at ends. Furthermore, the experimental dielectric constants and tunabilities are in good agreement with the calculated data, instructing that the dielectric properties of BST thin films with unchanged Ba/Sr ratio can be tailored by changing the structure to adjust the lattice misfit strain of each uniform layer. This implies that multilayer BST thin films also can be designed by phenomenological theory.

Introduction

In recent years, barium strontium titanate (BST) thin films as dielectric tunable materials exhibit strong dependence of dielectric constants under relative low voltage, having attracted much attention for the

development of tunable microwave applications, such as phase shifters, capacitors, and tunable oscillators [1–6]. For their applications in MEMS-structure tunable microwave devices, stainless steel (SS) substrate exhibits its advantages in low cost and integrating thin films with devices, exceeding the

Address correspondence to E-mail: jrcheng@staff.shu.edu.cn

performance of the conventional Si substrate [7–9]. SS substrate can act as bottom electrode and substrate at the same time, avoiding the complex micro-machined processes as the Si substrate. Besides, LaNiO_3 (LNO) conducting oxide with perovskite structure can be used as the buffer layer [9] to decrease the nucleation energy and lattice misfit strain for improving dielectric properties of perovskite structural ferroelectric thin films.

It has been reported that enhanced tunability for BST thin films on Pt/Si substrates could be achieved by building multilayer structures. A high tunability of 36.2 % under the electric field of 375 kV cm^{-1} can be obtained by sol-gel derived compositionally graded BST thin films [10]. Weiss et al. [11] have found that the tunability of MgO-doped BST multilayers can reach 29 % under the applied field of 444 kV cm^{-1} when the frequency is 10 GHz. Moreover, it is well known that lattice misfit stress and thermal misfit stress have great influences on the structures and dielectric properties of BST thin films. Ban et al. [12, 13] have theoretically analyzed the tunability of BST thin films using a phenomenological model, showing that the higher tunability can be obtained by adjusting misfit strain in the vicinity of a structural phase transformation. The tunability is also highly dependent upon thermal misfit strain of BST thin films [14]. However, seldom reports have investigated BST thin films with symmetrical multilayer structures by combining experimental process and phenomenological theoretical analyses.

In this paper, BST thin films with sandwich-like structure, which is the symmetrical multilayer structure, were deposited on LNO buffered SS substrates by sol-gel technique, and their structures, misfit strains, and dielectric properties were investigated. At the same time, misfit strains and dielectric tunabilities of such BST films were also theoretically carried out by a modified phenomenological model.

Experimental

Two kinds of sandwich-like structural BST thin films were fabricated by sol-gel technique on LNO buffered SS substrates: $\text{Ba}_{0.6}\text{Sr}_{0.4}\text{TiO}_3$ layer in the middle or at ends, as presented in Fig. 1 ($x = 0.3, 0.4, 0.5, 0.7,$ and 0.8 in $\text{Ba}_x\text{Sr}_{1-x}\text{TiO}_3$ layer). LNO precursor solution was prepared by using lanthanum nitrate hexahydrate [$\text{La}(\text{NO}_3)_3 \cdot 6\text{H}_2\text{O}$], nickel nitrate hexahydrate

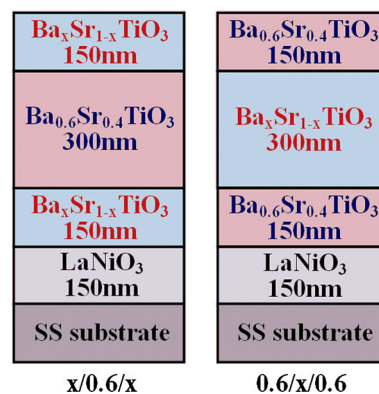


Figure 1 Schematic configurations of the two sandwich-like structures of BST thin films.

[$\text{Ni}(\text{NO}_3)_2 \cdot 6\text{H}_2\text{O}$], acetic acid, H_2O , and polyvinyl alcohol. Barium acetate [$\text{Ba}(\text{Ac})_2$], strontium acetate semihydrate [$\text{Sr}(\text{Ac})_2 \cdot 1/2\text{H}_2\text{O}$], and tetrabutyl titanate [$\text{Ti}(\text{OC}_4\text{H}_9)_4$] were used as raw materials, and acetic acid and 2-methoxy-ethanol were employed as solvents for BST precursor solution. The concentration of LNO and BST precursor solution was adjusted to 0.1 and 0.4 mol L^{-1} , respectively. Both LNO and BST precursor solutions were spin coated at 3000 rpm for 30 s and then were annealed at $550 \text{ }^\circ\text{C}$ for each layer. By repeating spin coating and annealing process several times, the thickness of LNO and BST layer was respectively reached according to the thickness shown in Fig. 1. Such BST thin films were finally annealing at $720 \text{ }^\circ\text{C}$ for 30 min.

The surface morphology was observed by field-emission scanning electronic microscope (FE-SEM, JEOL, JSM-7000F, Japan). The phase structure was characterized by X-ray diffraction (DLMAX-2200). Micro-Raman spectra (LABHR-UV) of the films were recorded with the 514.5 nm line of an Ar^+ laser. To measure the electric properties, Au top electrodes with 0.4 mm diameter were sputtered onto the surface of the films. The room temperature dielectric properties were measured by Agilent 4294A Precision Impedance Analyzer, and the applied voltage for tunability is 18 V ($\sim 300 \text{ kV cm}^{-1}$ for the films).

Phenomenological theoretical approach

Theoretical analyses are based on a Landau–Devonshire phenomenological model, in which thermodynamic potential is described as a function of polarization, applied electric field, and misfit strain.

Details for this model and the parameters of BST thin films can be found in some available references [12–17]. In our calculation, lattice misfit stress [12, 13], thermal misfit stress [14], and the effect of film thickness [12, 13] are considered at the same time. When lattice misfit stress is large, the corresponding lattice misfit strain for polycrystalline thin films can be relaxed by the in-plane formation of misfit dislocation. According to the ferroelectric critical grain size [18, 19] and the thickness of interface [20, 21], we assume that the largest relaxation range of lattice misfit stress is 20 nm and the relaxation range is linearly increased with the increased lattice misfit stress. In addition, LNO buffered SS substrate is regarded as a new substrate, which has the lattice parameter of LNO (~ 0.384 nm) and the thermal expansion coefficient (TEC) of SS ($\sim 17.8 \times 10^{-6} \text{ }^\circ\text{C}^{-1}$). According to the experimental process, the calculated dielectric constants and tunabilities are the out-of-plane dielectric responses, and the electric field for calculating tunabilities is

300 kV cm^{-1} . Besides, the interfaces in such BST thin films are neglected because their total thickness is much smaller than the thickness of the films.

Results and discussion

Morphology and structure

Schematic configurations of the two sandwich-like structures with varied average Ba/Sr ratio of BST thin films are shown in Fig. 1. Such BST films can be treated as the in-series connection of three uniform capacitor layers. As the symmetrical multilayer structures, both the composition and thickness of top layer and bottom layer are the same. Besides, the thickness of middle layer equals to the total thickness of top layer and bottom layer. Hence, when x is a constant, the average Ba/Sr ratio in the two structures is same.

Figure 2 presents the FE-SEM images of the surface of BST thin films, which mainly reflect the

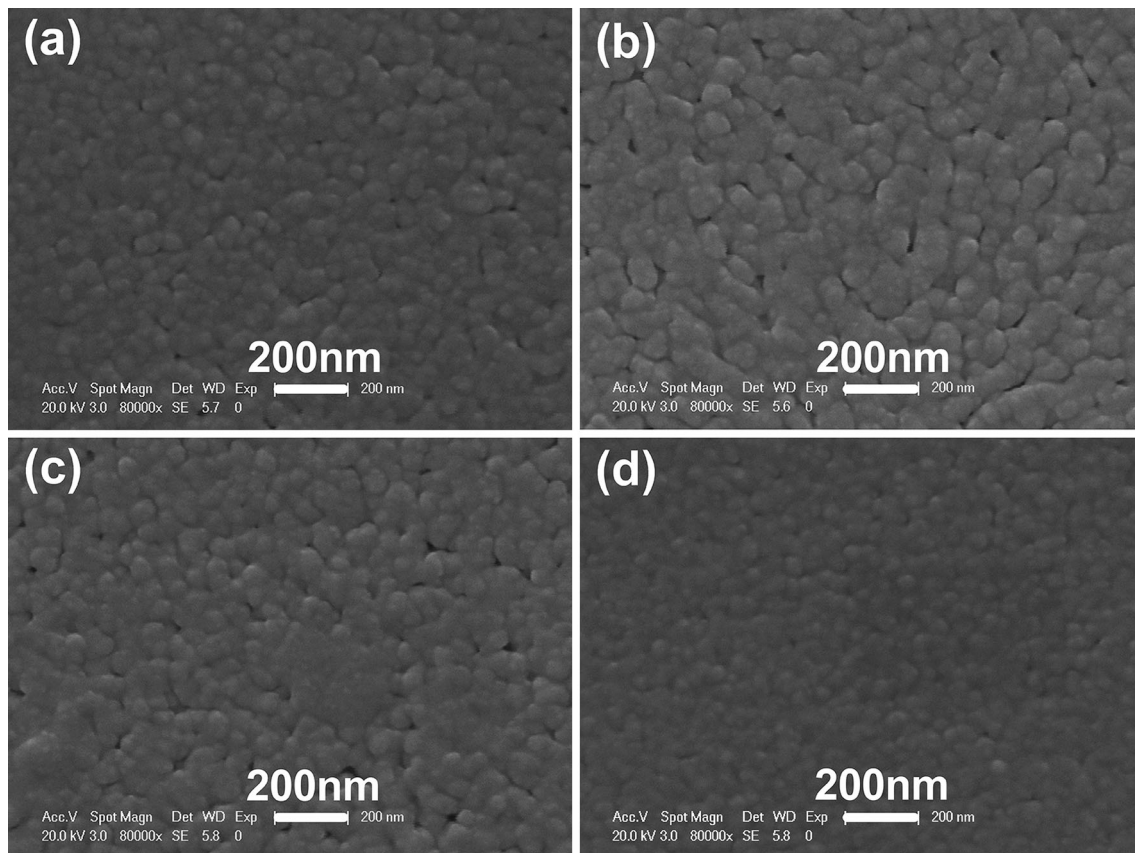


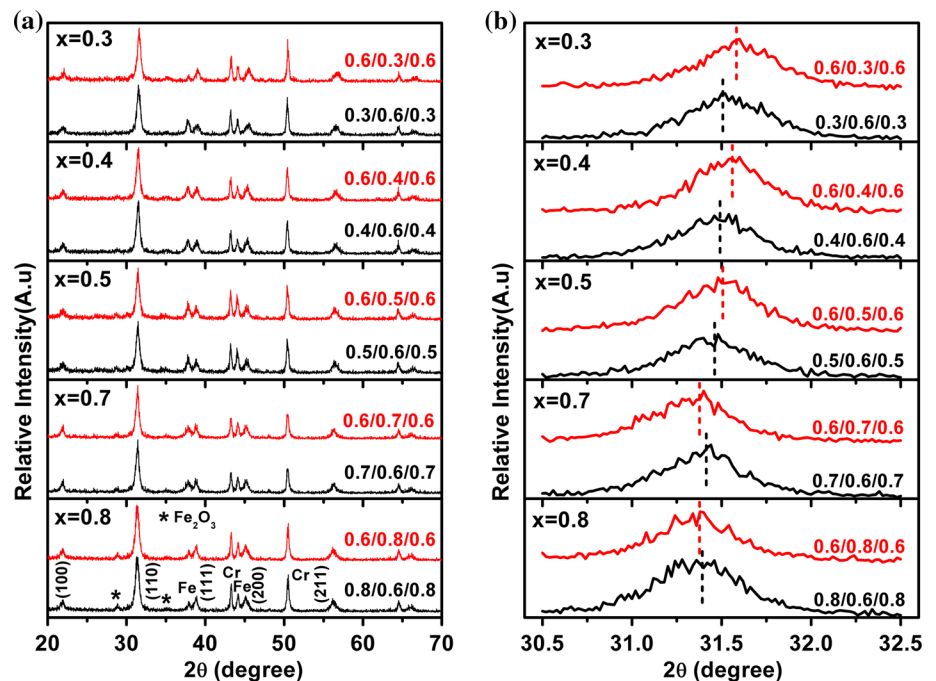
Figure 2 FE-SEM images of the surface of BST thin films: **a** $x = 0.4$ layers at ends, **b** $x = 0.4$ layer in the middle, **c** $x = 0.7$ layers at ends, **d** $x = 0.7$ layer in the middle.

morphology of top layer. It is observed that the surface of all samples is smooth, flat, and compact, suggesting their well grain growth. When the lattice parameter of top layer is smaller than that of middle layer, the top layer is effected by compressive lattice misfit stress; while on the contrary, the top layer is effected by tensile lattice misfit stress. Considering the compressive thermal misfit stress from SS substrates (the TEC of BST is smaller than that of SS), the top layer with larger lattice parameter is effected by smaller total misfit stress. And thus the nucleation energy of grain growth becomes smaller, leading to its easier grain growth and relatively larger grain size, as shown in Fig. 4b, c. The circumstance of the grain size in Fig. 4a, d is just on the contrary since the top layer is effected by larger total compressive misfit stress. Moreover, the average grain size of all samples is about 50–80 nm, much larger than the ferroelectric critical grain size [18, 19], and thus the possibility of different dielectric properties mainly resulting from grain size effect can be excluded.

X-ray diffraction (XRD) patterns of all samples and their (110) peaks are recorded in Fig. 3. It is seen from Fig. 3a that the major phase of all samples is the typical perovskite structure, indicating their well crystallization. The diffraction peaks of LNO buffer layer can not be found due to its relatively low content and weak peaks [9]. From Fig. 3b, it is noted that

the (110) peak is gradually shifted to low angle when increasing the average Ba/Sr ratio, because the ionic radius of Ba^{2+} ions is larger than that of Sr^{2+} ions and thus the lattice is enlarged. For same average Ba/Sr ratio of BST thin films, the position located by (110) peak also depends on the structures, suggesting that the strain of the films can be adjusted by the structures. BST thin films deposited on LNO buffered SS substrates are effected by total compressive misfit stress since the lattice parameter of LNO layer is smaller than that of BST films, and at the same time SS is a thermal “compressive” substrate. When increasing compressive misfit stress, the lattice of the films will be in-plane shrank but out-of-plane enlarged, and at last the volume of the lattice will be increased [12–14], leading the corresponding (110) peak to shift to lower angle. Therefore, when the average Ba/Sr ratio is unchanged, the structure shows higher angle of (110) peak meaning its smaller total compressive misfit strain. Meanwhile, it is found that the structure with smaller compressive misfit strain always has smaller lattice parameter of middle layer than that of top/bottom layer. For example, when $x = 0.4$, the films with the structure of $\text{Ba}_{0.6}\text{Sr}_{0.4}\text{TiO}_3$ layers at ends show higher angle of (110) peak, indicating that their compressive misfit strain is smaller than the films with the structure of $\text{Ba}_{0.6}\text{Sr}_{0.4}\text{TiO}_3$ layer in the middle.

Figure 3 XRD patterns of BST thin films (a) and their (110) peaks (b).



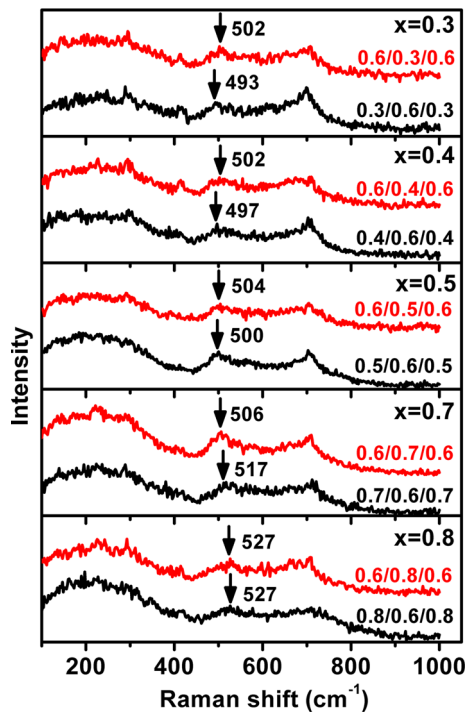


Figure 4 Raman spectra of all samples.

Figure 4 exhibits Raman spectra of all samples, which also can characterize their strains by observing the shift of peaks. The peak appeared at $\sim 500 \text{ cm}^{-1}$ is obviously seen, which is caused by the $A_1(\text{TO}_3)$ mode of Ti–O vibration in BST solid solutions [22, 23]. This peak shifts toward low frequency when decreasing the average Ba/Sr ratio in the films, which is also found in uniform BST ceramics or powders with little strain [22, 23]. This phenomenon indicates that the $A_1(\text{TO}_3)$ mode of Ti–O vibration will be depressed by the shrank lattice due to the smaller radius of Sr^{2+} ions. When increasing compressive stress upon the films with unchanged Ba/Sr ratio, the change of $A_1(\text{TO}_3)$ mode Ti–O vibration is considered to equal to the case of the little strained films with increased Sr^{2+} ions content. Therefore, for the unchanged average Ba/Sr ratio, higher frequency $A_1(\text{TO}_3)$ mode of the structure means its smaller compressive misfit strain. Thus, the strains examined by Raman spectra mainly agree with the above XRD results and analyses from Fig. 3b.

Dielectric properties

Dielectric properties of such BST thin films are presented in Fig. 5. It is observed that dielectric constant

and tunability of the films can be significantly tailored by changing the average Ba/Sr ratio and structures. When the average Ba/Sr ratio is unchanged, the structure with smaller lattice parameter of middle layer than that of top/bottom layer can achieve larger tunability resulting from its smaller compressive misfit strain, which has been analyzed from the above results of XRD and Raman spectra. This phenomenon is also theoretically found in BST thin films with uniform composition, as reported that BST thin films with a very small compressive misfit strain exhibit higher tunability and the tunability will decrease by increasing compressive misfit stress continually [12, 13]. Especially, by locating $\text{Ba}_{0.4}\text{Sr}_{0.6}\text{TiO}_3$ layer in the middle and $\text{Ba}_{0.6}\text{Sr}_{0.4}\text{TiO}_3$ layers at ends, the largest tunability of the films reaches 30.0 % under the electric field of 300 kV cm^{-1} , which is comparable to that of BST thin films deposited on the commonly used Pt/Ti/SiO₂/Si substrates [24–26].

Phenomenological theoretical analyses

Such sandwich-like structural BST thin films are also theoretically analyzed by the modified phenomenological model. Figure 6 shows the calculated total misfit strain of each uniform BST layer including lattice misfit strain and thermal misfit strain. All of the films are effected by total compressive misfit strain since the calculated misfit strain of each layer is below zero when $0.3 < x < 0.8$. This is because of the compressive lattice misfit stress from LNO layer and compressive thermal misfit stress from SS substrate. Moreover, it is obviously seen that the misfit strain in each uniform layer significantly depends on the structures when the average Ba/Sr ratio is same. For example, when $x = 0.4$, the misfit strain of top layer, middle layer, and bottom layer is -0.159 , -0.660 and -0.842 %, respectively, for the structure of $\text{Ba}_{0.6}\text{Sr}_{0.4}\text{TiO}_3$ layer in the middle; while for the structure of $\text{Ba}_{0.6}\text{Sr}_{0.4}\text{TiO}_3$ layers at ends, the corresponding misfit strain of each layer is -0.526 , -0.218 and -0.885 %, respectively. Such difference instructs that the lattice misfit strain of each uniform layer is adjusted by the structures because the structures can not change the thermal misfit strain caused by SS substrates. This probably leads to the different total misfit strains as found by above analyses from the results of XRD and Raman spectra. In addition, the calculated misfit strain for the top layer is in accordance with the analyses for FE-SEM images in Fig. 2

Figure 5 Dielectric properties of BST thin films: **a** dielectric constants, loss and tunabilities at 1 MHz, **b** dielectric constants as a function of frequency, **c** dielectric constants as a function of electric field at 1 MHz.

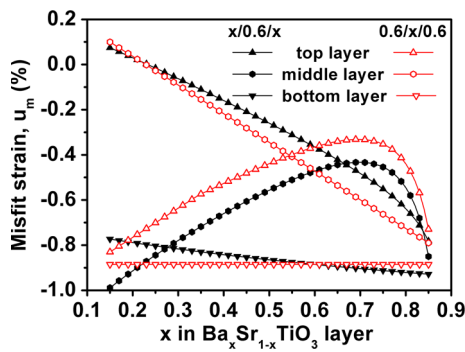
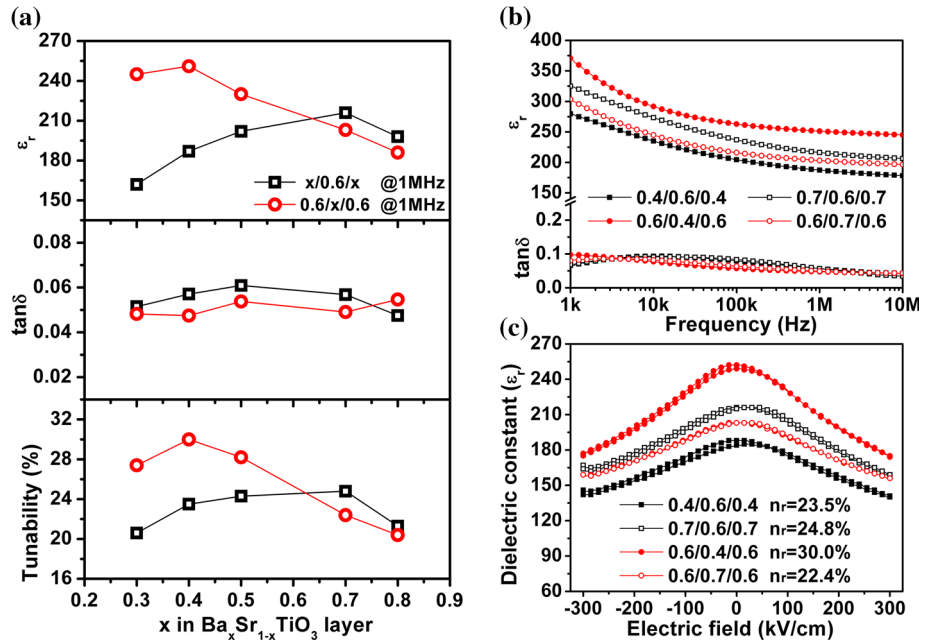


Figure 6 Calculated total misfit strain of each uniform layer for sandwich-like structural BST thin films.

that the top layer with larger lattice parameter than middle layer is effected by smaller total misfit stress.

Calculated dielectric constants and tunabilities of BST thin films are presented in Fig. 7. It is seen that the dielectric properties of the films significantly depend on the average Ba/Sr ratio and structures. And the regularity of tunability is clearer: when $x < 0.6$, the structure of $\text{Ba}_{0.6}\text{Sr}_{0.4}\text{TiO}_3$ layers at ends exhibits larger tunability than the structure of $\text{Ba}_{0.6}\text{Sr}_{0.4}\text{TiO}_3$ layer in the middle; when $x > 0.6$, the case is just on the contrary. This instructs that, for same average Ba/Sr ratio, the structure can achieve larger tunability when the lattice parameter of middle layer is smaller than that of top/bottom layer. The maximum of calculated tunability for the two structures of $\text{Ba}_{0.6}\text{Sr}_{0.4}\text{TiO}_3$ layer in the middle and at ends reaches 26.08 and 33.38 %

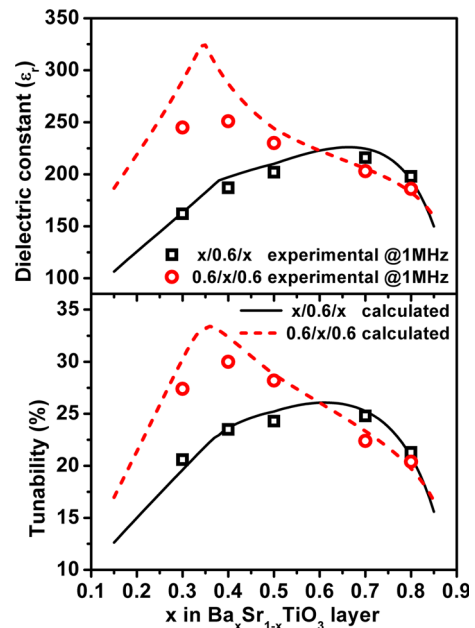


Figure 7 Calculated data and experimental results of dielectric constants and tunabilities of BST thin films.

under the electric field of 300 kV cm^{-1} , respectively, exceeding the performance of uniform $\text{Ba}_{0.6}\text{Sr}_{0.4}\text{TiO}_3$ thin films (when $x = 0.6$, the computed value is 26.07 %). Furthermore, it is noticed that the regularity and values of the measured dielectric constants and tunabilities are in good agreement with the results carried out by theoretical calculation, demonstrating that the dielectric properties of BST thin films with

unchanged average Ba/Sr ratio can be tailored by the structures because of the adjusted lattice misfit strain for each uniform layer, as presented in Fig. 6. This implies that general trends of dielectric properties for multilayer structure BST thin films also can be investigated by phenomenological theory.

Conclusions

In summary, two sandwich-like structures with varied average Ba/Sr ratio of BST thin films: $\text{Ba}_{0.6}\text{Sr}_{0.4}\text{TiO}_3$ layer in the middle or at ends, on LNO buffered SS substrates were prepared by sol–gel technique, and at the same time, were theoretically analyzed by a modified phenomenological model. It can be concluded that for same average Ba/Sr ratio, when middle layer shows smaller lattice parameter than top/bottom layer, the structure can achieve larger tunability because of its smaller total compressive misfit strain, which has been qualitatively examined by XRD and Raman spectra. By adjusting average Ba/Sr ratio and structures, the largest tunability can reach 30 % under the electric field of 300 kV cm^{-1} by locating $\text{Ba}_{0.4}\text{Sr}_{0.6}\text{TiO}_3$ layer in the middle and $\text{Ba}_{0.6}\text{Sr}_{0.4}\text{TiO}_3$ layers at ends. Moreover, the experimental dielectric constants and tunabilities are in accordance with the calculated results, instructing that the dielectric properties of BST thin films with same average Ba/Sr ratio can be tailored by the structure due to the adjusted lattice misfit strain of each uniform layer.

Acknowledgements

This work was supported by the National Natural Science Foundation of China (Grant No. 51302163) and the Innovational Foundation of Shanghai University (Grant. No. K.10- 0110-13-009).

Compliance with ethical standards

Conflict of interest In this paper, no conflicts of interest exist.

References

- [1] Kong LB, Li S, Zhang TS, Zhai JW, Boey FYC, Ma J (2010) Electrically tunable dielectric materials and strategies to improve their performances. *Prog Mater Sci* 55:840–893
- [2] Tagantsev AK, Sherman VO, Astafiev KF, Venkatesh J, Setter N (2003) Ferroelectric materials for microwave tunable applications. *J Electroceram* 11:5–66
- [3] Lee C-H, Orloff ND, Birol T, Zhu Y, Gian V, Rocas E et al (2013) Exploiting dimensionality and defect mitigation to create tunable microwave dielectrics. *Nature* 502:532–536
- [4] Stemme F, Brus M, GeBwein H, Schroeder M, Sazegar M, Drahus MD et al (2013) Fabrication and characterization of iron and fluorine co-doped BST thin films for microwave applications. *J Mater Sci* 48:3586–3596. doi:10.1007/s10853-013-7156-5
- [5] Sun X, Yang Y, Zhang Q, Zhou X, Zongzhi H, Huang C (2014) Enhanced dielectric and tunable properties of barium strontium titanate thin films through introducing $\text{Nd}(\text{Zn}_{1/2}\text{Ti}_{1/2})\text{O}_3$ and adjusting Ba/Sr. *J Mater Sci* 49:1058–1065. doi:10.1007/s10853-013-7783-x
- [6] Rouahi A, Kahouli A, Sylvestre A, Defay E, Yangui B (2012) Impedance spectroscopic and dielectric analysis of $\text{Ba}_{0.7}\text{Sr}_{0.3}\text{TiO}_3$ thin films. *J Alloys Comp* 529:84–88
- [7] Sharma AK, Gautam AK, Farinelli P, Dutta A, Singh SG (2015) A Ku band 5 bit MEMS phase shifter for active electronically steerable phased array applications. *J Micromech Microeng* 25:035014
- [8] Unlu M, Demir S, Akin T (2013) A 15–40-GHz frequency reconfigurable RF MEMS phase shifter. *IEEE Trans Microw Theory* 61:2865–2877
- [9] Huang S, Chen J, Cheng J (2015) Fabrication and characterization of compositionally graded $\text{Pb}_x\text{Sr}_{1-x}\text{TiO}_3$ thin films by the sol–gel method. *J Solgel Sci Technol* 73:278–282
- [10] Wang J, Xiang J, Bai L, TingzhiLiu GY, Zhang TJ (2008) Microstructure, dielectric and optical properties of compositionally graded $\text{Ba}_{1-x}\text{Sr}_x\text{TiO}_3$ thin film. *Mater Chem Phys* 112:542–545
- [11] Weiss CV, Okatan MB, Alpay SP, Cole MW, Ngo E, Toonen RC (2009) Compositionally graded ferroelectric multilayers for frequency agile tunable devices. *J Mater Sci* 44:5364–5374. doi:10.1007/s10853-009-3514-8
- [12] Ban Z-G, Alpay SP (2002) Phase diagrams and dielectric response of epitaxial barium strontium titanate films: a theoretical analysis. *J Appl Phys* 91:9288–9296
- [13] Ban Z-G, Alpay SP (2003) Optimization of the tunability of barium strontium titanate films via epitaxial stresses. *J Appl Phys* 93:504–511
- [14] Sharma A, Ban Z-G, Alpay SP, Mantese JV (2004) The role of thermally-induced internal stresses on the tunability of textured barium strontium titanate films. *Appl Phys Lett* 85:985–987
- [15] Khassaf H, Khakpash N, Sun F, Sbrockey NM, Tompa GS, Kalkur TS et al (2014) Strain engineered barium strontium

- titanate for tunable thin film resonators. *Appl Phys Lett* 104:202902
- [16] Zhong S, Alpay SP, Cole MW, Ngo E, Hirsch S, Demaree JD (2007) Highly tunable and temperature insensitive multilayer barium strontium titanate films. *Appl Phys Lett* 90:092901
- [17] Pertsev NA, Zembilgotov AG, Tagantsev AK (1998) Effect of mechanical boundary conditions on phase diagrams of epitaxial ferroelectric thin films. *Phys Rev Lett* 80:1988–1991
- [18] Chunlin F, Yang C, Chen H, Liye H, Wang Y (2005) Ferroelectric properties of $\text{Ba}_{0.6}\text{Sr}_{0.4}\text{TiO}_3$ thin films with different grain sizes. *Mater Lett* 59:330–333
- [19] Chen H, Yang C, Zhang J, Leng W, Ji H, Wang Z et al (2010) Two critical grain sizes of $\text{Ba}_{0.6}\text{Sr}_{0.4}\text{TiO}_3$ thin films. *J Mater Sci Mater Electron* 21:236–240
- [20] Sinnamon LJ, Bowman RM, Gregg JM (2001) Investigation of dead-layer thickness in $\text{SrRuO}_3/\text{Ba}_{0.5}\text{Sr}_{0.5}\text{TiO}_3/\text{Au}$ thin-film capacitors. *Appl Phys Lett* 78:1724–1726
- [21] Sinnamon LJ, Saad MM, Bowman RM, Gregg JM (2002) Exploring grain size as a cause for “dead-layer” effects in thin film capacitors. *Appl Phys Lett* 81:703–705
- [22] Zhang J, Zhai J, Chou X, Shao J, Xiang L, Yao X (2009) Microwave and infrared dielectric response of tunable $\text{Ba}_{1-x}\text{Sr}_x\text{TiO}_3$ ceramics. *Acta Mater* 57:4491–4499
- [23] Zhang Y, Chen C, Gao R, Xia F, Li Y, Che R (2015) Abnormal cubic-tetragonal phase transition of barium strontium titanate nanoparticles studied by in situ Raman spectroscopy and transmission electron microscopy heating experiments. *Appl Phys Lett* 107:182902
- [24] Liao J, Wei X, Ziqiang X, Wei X, Wang P (2012) The structure and dielectric properties of a novel kind of doped $\text{Ba}_{0.6}\text{Sr}_{0.4}\text{TiO}_3$ film. *Mater Chem Phys* 135:1030–1035
- [25] Radhapiyari Laishram SK, Pandey OP, Thakur DKB (2013) Dielectric and optical properties of $\text{Ba}_{0.6}\text{Sr}_{0.4}\text{Ti}_{0.99}\text{Fe}_{0.01}\text{O}_3$ thin films deposited by pulsed laser deposition technique for microwave tunable devices. *J Alloys Compd* 579:205–208
- [26] Tarale AN, Sutar MM, Salunkhe DJ, Joshi PB, Kulkarni SB, Pawar RC et al (2013) Dielectric properties of sol-gel synthesized $\text{SrTiO}_3/(\text{Ba}_{0.7}\text{Sr}_{0.3})\text{TiO}_3$ and $\text{SrTiO}_3/\text{Ba}(\text{Zr}_{0.3}\text{Ti}_{0.7})\text{O}_3$ thin film heterostructures. *J Mater Sci Mater Electron* 24:1308–1318